Membrane Topology of the Di- and Tripeptide Transport Protein of *Lactococcus lactis*†

Anja Hagting, Joeke v. d. Velde, Bert Poolman,* and Wil N. Konings

Department of Microbiology, Groningen Biomolecular Sciences and Biotechnology Institute, Kerklaan 30, 9751 NN Haren, The Netherlands

Received December 13, 1996; Revised Manuscript Received March 31, 1997⊗

ABSTRACT: Transport of hydrophilic di- and tripeptides into *Lactococcus lactis* is mediated by a proton motive force-driven peptide transport protein (DtpT) that shares similarity with eukaryotic peptide transporters, e.g., from kidney and small intestine of rabbit, man, and rat. Hydropathy profiling in combination with the "positive inside rule" predicts for most of the homologous proteins an α-helical bundle of 12 transmembrane segments, but the positions of these transmembrane segments and the location of the amino and carboxyl termini are by no means conclusive. The secondary structure of DtpT was investigated by analyzing 42 DtpT−alkaline phosphatase fusion proteins, generated by random or directed fusions of the corresponding genes. These studies confirm the presence of 12 transmembrane segments but refute several other predictions made of the secondary structure. Data obtained from the fusion proteins were substantiated by studying the accessibility of single cysteine mutants in putative cytoplasmic or extracellular loops by membrane (im)permeant sulfhydryl reagents. The deduced topology model of DtpT consists of a bundle of 12 α-helixes with a short amino and a large carboxyl terminus, both located at the cytoplasmic site of the membrane. On the basis of sequence comparisons with DtpT, it seems likely that the structure model of the amino-terminal half of DtpT also holds for the eukaryotic peptide transporters, whereas the carboxyl-terminal half is largely different.

The di- and tripeptide transport system (DtpT)[1] of *Lactococcus lactis* is an integral membrane protein that mediates transport of hydrophilic di- and tripeptides in symport with protons. Transport of the more hydrophobic di- and tripeptides is catalyzed by another di- and tripeptide transport system DtpP (Foucaud et al., 1995). This transport is ATP-driven, like the uptake of peptides of more than three amino acid residues via the oligopeptide transport system Opp (Kunji et al., 1995). Like other known prokaryotic peptide transporters for which gene sequences are available, the Opp system, and most likely DtpP as well, belongs to the ATP-binding cassette (ABC) superfamily of transport proteins, also referred to as traffic ATPases (Higgins, 1992). In contrast to these binding protein-dependent transport systems, the di- and tripeptide carrier DtpT of *L. lactis* is driven by the proton motive force and composed of a single polypeptide of 463 amino acid residues. The DtpT protein has been shown to be homologous to peptide transport proteins of *Saccharomyces cerevisiae* (PTR2) (Perry et al., 1994), *Arabidopsis thaliana* (AtPTR2A and AtPTR2B) (Steiner et al., 1994; Song et al., 1996), rabbit intestine (rbPepT1) (Fei et al., 1994), human intestine (hPepT1) (Liang et al., 1995), and *Candida albicans* (CaPTR2) (Basrai et al., 1995), as well as a nitrate transport protein of *A. thaliana* (AtCHL) (Tsay et al., 1993); this group of proteins has been designated the peptide transport (PTR) family (Steiner et al., 1995). Alignment of the eukaryotic proteins revealed a high number of identical and similar residues, and conserved glycosylation and phosphorylation sites, as well as a signature sequence unique to this group of proteins. The similarity of the eukaryotic proteins with DtpT is lower and mainly confined to the N-terminal half. Recently, other genes encoding eukaryotic peptide transporters [i.e., from kidney and intestine of rabbit, rat, and man (Boll et al., 1996; Liu et al., 1995; Miyamoto et al., 1996)] that share characteristics of the PTR family have been described. The transport proteins PepT2 of rabbit and human kidney have been shown to function as peptide-H^+ symporters (Boll et al., 1996; Liu et al., 1995).

Polytopic cytoplasmic membrane proteins span the membrane in a zigzag manner; the transmembrane segments (TMSs) are usually predicted to be in an α-helical configuration. The orientation of TMSs is, at least in part, determined by the distribution of the charged residues near the ends of TMSs. von Heijne has pointed out that short cytoplasmic loops have more basic residues than would be expected from a random distribution in hydrophilic regions of membrane proteins (von Heijne & Gavel, 1988). Thus, inspection of the aligned sequences and the use of algorithms to identify membrane-spanning regions allow the construction of topological models.

To test these models, we have made and analyzed gene fusions between *dtpT* and *phoA*. To support the data obtained from the protein fusion approach, single cysteine residues were engineered at selected places in DtpT, and their accessibility to membrane-impermeant sulfhydryl reagents was measured. Overall, the results suggest that the predicted models need adjustment, especially with regard to the

† This work was supported by a grant from the BRIDGE-T project of the EC-Science Foundation Programme (Contract BIOT-CT91-0263).

* Corresponding author. Telephone: +31 50 3632170. Fax: +31 50 3632154. E-mail: B.Poolman@biol.rug.nl.

⊗ Abstract published in *Advance ACS Abstracts,* May 15, 1997.

[1] Abbreviations: DTT, dithiothreitol; LacZ, β-galactosidase; MPB, 3-(*N*-maleimidylpropionyl)biocytin; PhoA, alkaline phosphatase; AMdiS, 4-acetamido-4′-maleimidylstilbene-2,2′-disulfonic acid; SDM, site-directed mutagenesis; TMS, transmembrane-spanning segment; X-Gal, 5-bromo-4-chloro-3-indolyl β-D-galactopyranoside; XP, 5-bromo-4-chloro-3-indolyl phosphate; $DtpT_{LL}$ and $DtpT_{LH}$, di- and tripeptide protein of *Lactococcus lactis* and *Lactobacillus helveticus*, respectively.

S0006-2960(96)03068-1 CCC: $14.00

Table 1: Oligonucleotides Used for Mutagenesis and Sequencing of the Di- and Tripeptide Transport Gene of *L. lactis*[a]

primer	mutagenic oligonucleotide	characteristics
PhoAfor	5′-CGC**GGATCC**CG**GAGCTCCCGGG**CCTGTTCTGGAAAAC	*Bam*HI, *Sac*I, *Sma*I
PhoArev	5′-CG**GGATCCTCGAGCCATGG**TTGCTAACAGCA	*Bam*HI, *Xho*I, *Nco*I
DtpTfor3	5′-ACCTTGAA**AAGCTT**GTTATTGT	*Hin*dIII
PhoA1	5′-CGCAGAGCGGCAGTCTG	
DtpTfor6	5′-CATCTT**GGTACC**AATTG	*Kpn*I
DtpTrev5	5′-CAAGA**GGATCC**TCAGGAGC	*Bam*HI
DtpTcystC	5′-TTGAATGGG**TGT**TCTGGACGT	T360C
DtpTcystE	5′-TCAACAAAA**TGT**GCGCCAGTA	L394C
DtpTcystF	5′-ACACCTATC**TGT**AAAGCAGCA	F425C
DtpTcystG	5′-ATGGGAGATTGTCGTTAATTA	V462C

[a] Nucleotides in boldface correspond to a restriction site or cysteine mutant.

location and/or orientation of the TMSs at the extremities of the protein. The activities of the DtpT−reporter fusion proteins and the pattern of labeling of the cysteine residues are consistent with a secondary structure model that consists of 12 TMSs with both N and C termini located intracellularly.

EXPERIMENTAL PROCEDURES

Bacterial Strains and Growth Conditions. *Escherichia coli* CC118 (*ara* D139Δ) [*ara leu*] 7697 Δ*lac* X74 Δ*phoA* 20 *gal*E *gal*K *thi rsp*E *rpo*B *arg*E-[am], *rec*AI) (Calamia & Manoil, 1990) cells were grown at 37 °C, with vigorous aeration, in Luria Broth supplemented with carbenicillin (50 μg/mL) when appropriate. The chromogenic reagent 5-bromo-4-chloro-3-indolyl phosphate (XP) was used as an indicator of alkaline phosphatase activity and was added at 40 μg/mL to Luria Broth agar plates. *L. lactis* AG300 cells were grown on a chemicaly defined medium (Poolman & Konings, 1988) at pH 6.4, supplemented with erythromycine (5 μg/mL), plus 1% (w/v) glucose.

General DNA Manipulations. Plasmid DNA was prepared by the alkaline lysis method as described by Sambrook et al. (1989). Restriction enzyme digestions were carried out according to the manufacturer's recommendations. Ligation of DNA fragments and transformation were performed as described by Sambrook et al. (1989). For the exact localization of the random fusion points and confirmation of the sequence of PCR-amplified DNA, the DNA was sequenced by the dideoxy chain termination method (Sanger et al., 1977) using T7 DNA polymerase. PCR was performed with VENT DNA polymerase (New England Biolabs). After 35 cycles of amplification, the PCR products were purified using the QIAquick spin PCR purification kit (Qiagen).

Construction of pDT32 and Generation of Random dtpT−phoA Fusions. Plasmid pDT32 was constructed from pDT3 (Hagting et al., 1994), which contains the *dtpT* gene under control of its own promoter. The *phoA* gene from plasmid pPHO7 (Gutierrez & Devedjian, 1989) was amplified by PCR using the forward primer, PhoAfor, containing a *Bam*HI, *Sac*I, and *Sma*I site, and the reverse primer, PhoArev, containing a *Bam*HI, *Xho*I, and *Nco*I site (Table 1). The amplified *phoA* gene was restricted with *Bam*HI and *Xho*I and ligated into *Bam*HI−*Sal*I-digested pDT3. Random *dtpT−phoA* fusions were constructed as follows. *Sac*I−*Bam*HI-digested pDT32 was further digested with exonuclease III to create deletions from the 3′ end of *dtpT*. Subsequently, the DNA was blunt-ended with S1 nuclease and ligated. The ligation mixture was transformed to competent *E. coli* CC118 cells and plated on LB plates supplemented with 50 μg/mL carbenicillin plus 40 μg/mL XP. *dtpT−phoA* fusions were identified as blue colonies. Plasmid DNA was isolated, and after restriction analysis, the fusion point was determined by sequencing using oligonucleotide PhoA1 (Table 1).

Generation of Site-Specific dtpT−phoA Fusions. Site-specific *dtpT−phoA* fusions were made using PCR-amplified *dtpT* DNA. For construction of the *dtpT−phoA* fusions, DtpTfor3 primer, containing a *Hin*dIII site, was used in combination with several reverse primers that contain a *Bam*HI restriction site after the codons of interest. The second multiple cloning site of pPHO7 was removed as a *Xho*I−*Sac*I fragment, yielding pPHO7A. After restriction with *Hin*dIII and *Bam*HI, the PCR fragments were ligated into pPHO7A. The ligation mixtures were used to transform competent *E. coli* CC118 cells, which were plated on LB plates containing carbenicillin (50 μg/mL) plus XP (40 μg/mL). Plasmid DNA was isolated and sequenced using oligonucleotide PhoA1.

Enzyme Assays. Alkaline phosphatase (PhoA) activities were assayed essentially as described (Brickman & Beckwith, 1975). For growth of *E. coli* cells harboring *dtpT−phoA*, single colonies were diluted into 4 mL of LB containing 50 μg/mL carbenicillin and grown until A_{660} was 0.2−0.7. For PhoA activities, 1 mL of each culture was centrifuged and resupended in 1.5 mL of 1 M TRIS-HCl (pH 8.0). The A_{660} was measured, and 50 μL of 0.1% SDS and 50 μL of chloroform were added to 1 mL of the cell suspension. The tubes were vortexed and incubated for 5 min at 30 °C to permeabilize the cells. The PhoA assay was started by the addition of 0.1 mL of 0.4% (w/v) *p*-nitrophenyl phosphate (Sigma) and stopped by the addition of 0.2 mL of 1 M potassium hydrogen phosphate. PhoA activity units were calculated from the absorbance at 420 nm ($A_{420} - 1.75A_{550} \times 1000$)/[time(min) × A_{660} × volume of the culture assayed (mL)]. All activity values shown are the result of at least three independent assays; on average, the alkaline phosphatase activities in these assays varied less than 20%.

Immunoblotting. Part of the samples used for PhoA activity measurements was subjected to SDS−polyacrylamide electrophoresis using 10% polyacrylamide (the samples were boiled for 5 min in sample buffer prior to loading onto the gel), after which the proteins were transferred to polyvinylidene difluoride (PVDF; Millipore) sheets by semi-dry electroblotting (Kyhse-Anderson, 1984). PhoA hybrid proteins were detected using a mouse anti-*E. coli* alkaline phosphatase monoclonal antibody (Chemicon International Inc.); alkaline phosphatase-coupled goat anti-mouse IgG was used as a secondary antibody (Sigma).

Construction of Cysteine Mutants of DtpT. Oligonucleotide-directed site-specific mutagenesis was used to generate single cysteine residues in DtpT; the wild-type DtpT protein is devoid of cysteines. Cys replacement mutants were constructed by a two-step PCR method. The synthetic mutagenic primers used are given in Table 1. The oligonucleotides DtpTrev5 and DtpTcystC, -E, -F, or -G were used as primers in the first PCR step with plasmid pGKHT as the template. The pGKHT vector contains the *dtpT* gene with additional codons at the 3′ end that specify a six-histidine tag (A. Hagting et al., unpublished results). Subsequently, the PCR products were used as a primer in the second PCR with oligonucleotide DtpTfor6 and plasmid pGKHT as the template. The resulting 571 bp fragments were digested with *Kpn*I and *Bam*HI and exchanged with the equivalent fragment of pGKF52. pGKF52 is a derivative of pGKF5 (Hagting et al., 1994), in which an approximately 0.8 kb *Eco*RI−*Nco*I fragment has been deleted to remove the *Kpn*I site in the multiple cloning site. The 1180 bp *Eco*RI−*Kpn*I and 571 bp *Kpn*I−*Bam*HI fragments of the mutants were checked by nucleotide sequencing.

Labeling with 3-(N-Maleimidylpropionyl)biocytin. L. lactis AG300 cells (Hagting *et al*., 1994), expressing the desired plasmid contruct, were grown on a chemically defined medium (Poolman & Konings, 1988), supplemented with erythromycine (5 μg/mL) plus 1% (w/v) glucose, and harvested at the end exponential phase ($A_{660} \sim 0.8$). Cells were washed once with buffer B [50 mM potassium phosphate (pH 7.5) supplemented with 5 mM $MgSO_4$], deenergized with 20 mM deoxyglucose for 30 min at 30 °C, and subsequently washed twice with buffer B. Part of the cells was incubated with 200 μM 4-acetamido-4′-maleimidylstilbene-2,2′-disulfonic acid (AMdiS, Molecular Probes Inc.) at 30 °C for 30 min to block externally exposed cysteine residues, followed by two washing steps. AMdiS-treated and untreated cells were incubated with 100 μM 3-(*N*-maleimidylpropionyl)biocytin (MPB, Molecular Probes Inc.) for 10 min at 30 °C. MPB was added from a 20 mM stock prepared in dimethyl sulfoxide. The labeling was stopped by the addition of 10 mM dithiothreitol (DTT), and the cells were washed twice with buffer B. The cells were resuspended at an A_{660} of approximately 50 and treated with 5 mg/mL lysozyme for 30 min at 30 °C. Subsequently, the protoplasts were sonicated at an amplitude of 6 μm, using five cycles of 15 s of sonication and 45 s rest, at 4 °C under a constant stream of N_2. The mixture was centrifuged (15000*g*, Eppendorf centrifuge, 15 min), and the supernatant was collected. The membranes were pelleted by centrifugation (280000*g*, 15 min) and resuspended in buffer B. For maximal labeling with MPB, the probe was added to the cells prior to sonication; further conditions and handlings were the same as described above.

The His tag at the C terminus of DtpT was used to partially purify the DtpT protein. Membranes (2 mg/mL protein) were solubilized in buffer A [50 mM potassium phosphate (pH 8.0), 10% (v/v) glycerol, and 200 mM NaCl] with 1% (w/v) *n*-dodecyl maltoside for 30 min on ice. The insoluble material was removed by centrifugation (280000*g*, 15 min), and the supernatant was mixed and incubated with Ni-NTA (nitrilotriacetic acid) resin that was equilibrated with buffer A containing 0.1% (w/v) *n*-dodecyl maltoside. The Ni-NTA resin was washed with buffer A containing 0.1% (w/v) *n*-dodecyl maltoside plus 15 mM imidazole. The protein was eluted with buffer A, containing 0.1% (w/v) *n*-dodecyl maltoside plus 100 mM imidazole, subjected to SDS−PAGE, and transferred onto PVDF membranes by semidry electroblotting. Biotinylated proteins were detected using streptavidin-conjugated alkaline phosphatase (Boehringer Mannheim); DtpT protein was detected by anti-DtpT polyclonal antibodies using an alkaline phosphatase-coupled goat anti-mouse IgG (Sigma) as a secondary antibody.

Transport Assays. [^{14}C]Prolylalanine uptake in *L. lactis* AG300 cells, expressing DtpT cysteine mutants, was measured as previously described (Hagting et al., 1994).

RESULTS

Prediction of the Membrane Topology of the DtpT Protein. Using the algorithm of Eisenberg et al. (1984), 12 membrane-spanning regions were predicted by the hydropathy profiling. A secondary structure model of DtpT based on the hydropathy profile (Figure 1A) and the positive inside rule suggests a 12-helix bundle protein with the amino and carboxyl termini located at the outer surface of the membrane (Figure 1B). Other hydropathy profiling methods [e.g., Klein et al. (1985)] yielded secondary structure models in which the locations of the transmembrane segments in the N-terminal part were predicted differently. To test these models, *dtpT−phoA* gene fusions were constructed.

Construction and Analysis of Randomly Generated dtpT−phoA Fusions. The nested-deletion method was used to generate gene fusions encoding hybrid proteins with different portions of the DtpT protein joined to the amino terminus of alkaline phosphatase. The resulting plasmids were transformed to *E. coli* CC118 cells (PhoA$^-$), and blue colonies were selected on plates containing the chromogenic substrate 5-bromo-4-chloro-3-indolyl phosphate (XP). The gene fusions from 23 blue colonies were all found to be in-frame and corresponded to different portions of DtpT; the fusion proteins were named by the last amino acid codon number of DtpT before the fusion point. Plasmid DNA of a number of white colonies was isolated, and after restriction analysis, the fusion points were mapped by nucleotide sequencing, but only out-of-frame fusions were detected. The fusion points in the plasmids isolated from the blue colonies were not as randomly distributed as expected (Figure 1B, circles). For instance, no fusion proteins were found in the middle or the C-terminal part of the DtpT protein. When the fusion proteins were investigated for alkaline phosphatase activity (Table 2), the majority exhibited relatively high levels of activity as anticipated from their phenotype on XP plates. The fusion constructs S41, T67, and L343 had PhoA activities that were lower than expected from their blue appearance on XP plates. It should be stressed, however, that the activity was measured in cells that were harvested at the exponential phase of growth whereas the plate assay corresponded to stationary phase cells in which the activity may be higher (van Geest & Lolkema, 1996). All fusion proteins that had a PhoA activity of >75 are indicated by filled circles. The fusion proteins that had a quite low activity, but higher than the control, are indicated by open circles. Clearly, the position of the fusions in the secondary structure model suggests the need of major adjustments in the N-terminal part of the DtpT protein.

E. coli CC118 cells harboring the plasmids with the *dtpT−phoA* fusions were subjected to immunoblotting, and hybrid

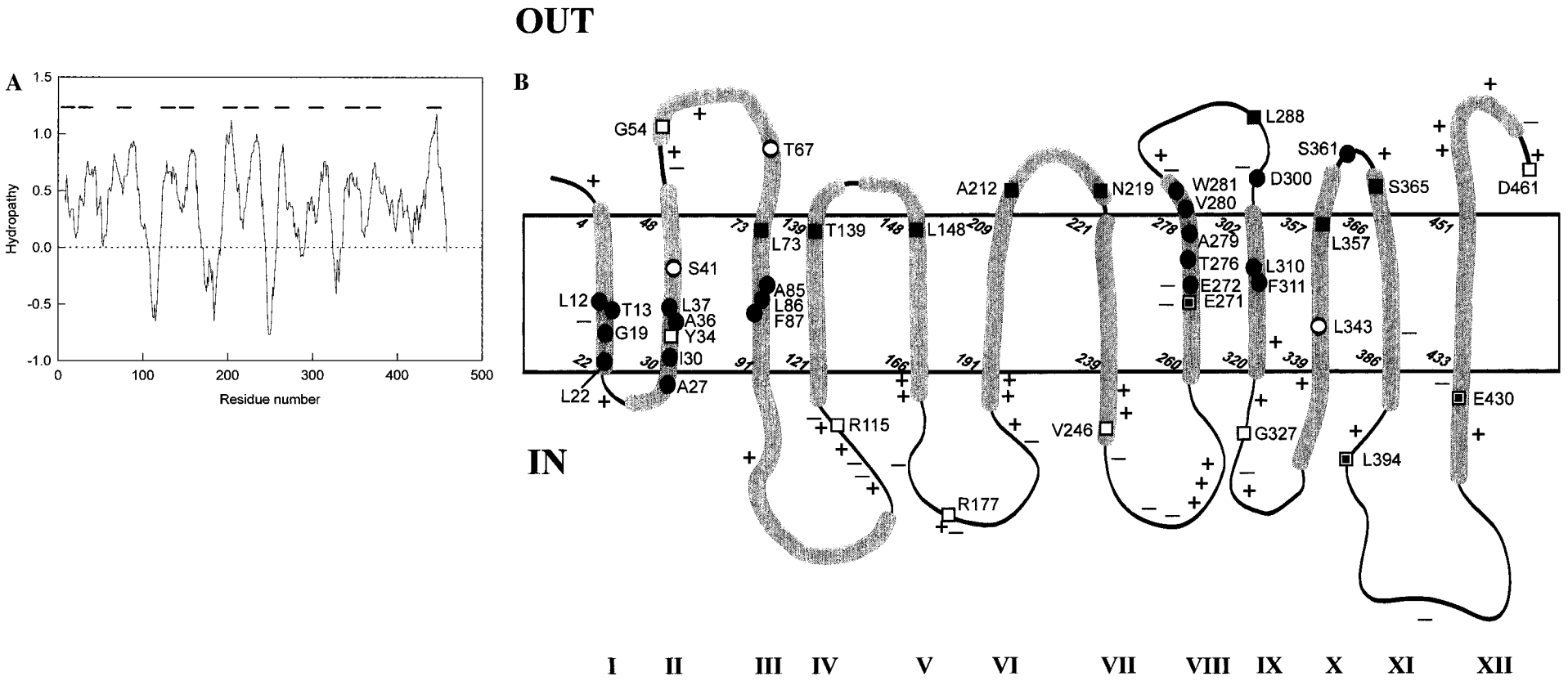

FIGURE 1: Hydropathy profile (A) and a secondary structure model of the di- and tripeptide transport protein of *L. lactis* (B). The hydropathy profile was obtained by using the algorithm of Eisenberg et al. (1984) with a sliding window of 13 residues; the predicted TMSs are indicated as solid lines above the plot. The hydropathy profile and the "positive inside rule" (von Heijne & Gavel, 1988) were used to construct the model. For the distribution of positive charges, histidine residues were not taken into account. Circles indicate the position of the randomly generated PhoA fusions. ● and ○ correspond to high (>75 units) and low alkaline phosphatase activity (<75 units), respectively. Squares (■, box with solid square inside, and □ represent high, intermediate, and low alkaline phosphatase activity, respectively) depict DtpT−PhoA fusion proteins that were constructed by SDM. The shaded stretches indicate the maximum length of a TMS with an overall hydrophobicity of ≥0.5 (based on the algorithm of Eisenberg using a sliding window of 19). Charged residues are indicated: +, K and R; −, D and E.

Table 2: Alkaline Phosphatase Activity of Randomly Generated DtpT−PhoA Hybrid Proteins[a]

fusion[a]	PhoA activity	fusion[a]	PhoA activity
L12	127	F87	404
T13	135	E272	278
G19	152	T276	626
L22	287	A279	459
A27	473	V280	823
I30	400	W281	343
A36	614	D300	806
L37	306	L310	300
S41	60	F311	267
T67	12	L343	16
A85	577	S361	163
L86	550	vector control	2

[a] Amino acid in the DtpT protein that precedes the fusion point.

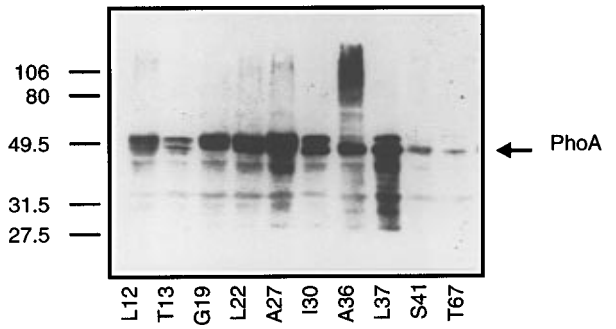

FIGURE 2: Immunoblot analysis of randomly generated DtpT−PhoA chimeras. *E. coli* CC118 cells containing the plasmids encoding DtpT−PhoA fusion proteins were grown in LB containing 50 μg/mL carbenicillin. The total cell protein (30 μg) was subjected to 10% SDS−PAGE, electroblotted, and visualized as described in Experimental Procedures.

proteins were detected using a monoclonal anti-PhoA antibody. These experiments were performed with the same batch of *E. coli* CC118 cells that were used to measure the alkaline phosphatase activity. In each case, the major band reacting with the anti-PhoA antibody comigrated with a molecular mass of approximately 50 kDa, which correlates with the size of native alkaline phosphatase. In the case of L12, T13, I30, L37 (Figure 2), A212, and N219 (not shown), doublet bands the size of native alkaline phosphatase and the corresponding fusion protein were observed. Comparison of immunoblot data and the activity measurements (Table 2) indicate that the differences in activity correlate, at least qualitatively, with variation in expression. It should be stressed that the activity measurements (e.g., Table 2) represent the average of three independent experiments, whereas only the samples of a single experiment are shown in Figure 2.

Construction and Analysis of Site-Specific dtpT−phoA Fusions. Since the range of fusions obtained by the nested-deletion method was unsatisfactory, additional site-specific fusions with alkaline phosphatase were constructed. To construct these fusions, the corresponding 5′ region of the *dtpT* gene was amplified by PCR and ligated, in-frame, with the *phoA* gene. The alkaline phosphatase activity of the 19 DtpT−PhoA fusion proteins varied from 3 to 386 units (Table 3); the fusions are indicated as squares in Figure 1B (and Figure 4, see below). Immunodetection of the fusion proteins with high activity revealed, in most cases, proteolytic degradation products the size of native alkaline phosphatase. In general, full length chimeras or degradation products were barely or not detectable with low-activity fusions [as observed by others; e.g., Pourcher et al.(1996)].

Table 3: Alkaline Phosphatase Activities of the DtpT−PhoA Hybrid Proteins Generated by Site-Specific Mutagenesis

	PhoA activity			PhoA activity	
fusion[a]	units	class[b]	fusion[a]	units	class[b]
Y34	18	L	L260	4	L
G54	7	L	E271	48	I
L73	353	H	L288	125	H
R115	12	L	G327	3	L
T139	386	H	L357	98	H
L148	211	H	S365	242	H
R177	14	L	L394	71	I
A212	210	H	E430	32	I
N219	188	H	D461	4	L
V246	19	L	vector	2	L

[a] Last amino acid in the DtpT protein that precedes the fusion point. [b] H, I, and L indicate high (PhoA of >75 u), intermediate (PhoA between 25 and 75 u), and low (PhoA of <25 u) activities, respectively.

The results obtained with the fusion proteins with their junction point in the middle part of the protein (putative helices IV−XI, Figure 1B) are in good agreement with the predicted structure. However, the model needs adjustment in the N- and C-terminal parts of the protein. Using the algorithm of Klein et al. (1984), a TMS from residue 58 to 74 is predicted, whereas residues 3−21 are not predicted to form a TMS. The existence of these two TMSs is strongly suggested by the analysis of the DtpT−PhoA fusions. The results obtained with the chimeric proteins L394, E430, and D461 indicate that the model also needs revision in the C-terminal part of the DtpT protein. One possibility would be that the putative membrane-spanning segment XII is not crossing the membrane but is located in the cytoplasm. To test this hypothesis, single cysteine residues were engineered in the C-terminal part of the DtpT protein and their accessibility to membrane-(im)permeant sulfhydryl reagents was measured.

Biotinylation of Cysteine Residues. Since wild-type DtpT does not have cysteine residues, cysteines engineered in putative extracellular or cytoplasmic loops can be used to determine the membrane sideness of these regions upon labeling with membrane-impermeant sulfhydryl reagents. 3-(*N*-Maleimidylpropionyl)biocytin (MPB) is a thiol-specific compound that may slowly cross the membrane and thereby label internal and external cysteines, i.e., when used at relatively high concentrations and/or long incubation times (Bayer et al., 1985; Loo & Clarke, 1995). 4-Acetamido-4′-maleimidylstilbene-2,2′-disulfonic acid (AMdiS) possesses two charged sulfonate groups which makes this probe highly membrane-impermeable. When single cysteine mutants are treated with AMdiS, prior to incubation with MPB, cysteines located in extracellular loops should not become labeled by MPB, contrary to residues in internal loops. This approach is even more powerful than the analysis of fusion proteins when it can be shown that the mutants retain their native structure, for which retention of function is the best indication. Uptake experiments confirmed that all mutants take up radiolabeled prolylalanine at a rate similar to that of wild-type DtpT (data not shown). To study the membrane topology, the cysteine mutants were treated with MPB, with or without pretreatment with AMdiS. After partial purification, the His-tagged proteins were subjected to SDS−PAGE and immunoblotting, and the amount of DtpT protein was

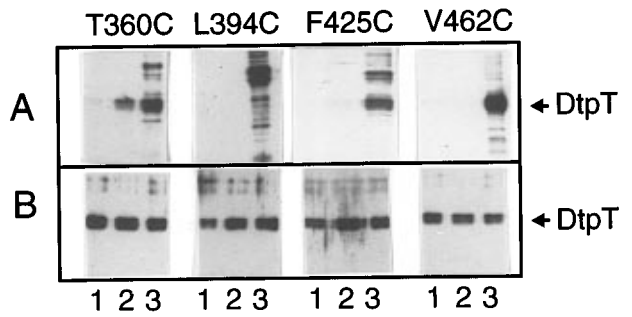

FIGURE 3: Labeling and immunological detection of DtpT Cys mutants. *L. lactis* AG300 cells carrying plasmids containing the single cysteine mutants of *dtpT* were labeled with MPB with (1) or without (2) pretreatment with AMdiS. To make intracellularly located cysteines accessible for the maleimide, the cells were sonicated in the presence of MPB (3). The partially purified DtpT proteins were subjected to SDS−PAGE, electroblotted, and visualized by streptavidin-conjugated alkaline phosphatase (A) or anti-DtpT polyclonal antibodies (B).

determined with an anti-DtpT polyclonal antibody. The variations in the amount of DtpT were less than 2-fold (Figure 3B). Figure 3A shows that cells expressing mutant T360C were biotinylated (lane 2) and that the biotinylation of this mutant was blocked by pretreatment with AMdiS. These results are consistent with T360C being located at the extracellular surface. By contrast, biotinylation of whole cells expressing mutants L394C, F425C, and V462C was barely or not detectable. To test whether these cysteines can react with MPB, the cells were sonicated prior to labeling. Biotinylation of the mutants T360C, F425C, and V462C was detected (Figure 3, lanes 3), whereas mutant L394C was not accessible to labeling by MPB. The lack of biotinylation of F425C and V462C in intact cells can be due to slow membrane penetration of MPB into the cells and/or to a decrease of the free MPB concentration at the inside as a result of reaction with intracellular thiol compounds. In both cases, the data strongly suggest that these residues are located at the cytoplasmic face of the membrane. This confirms the suggestion that the last putative membrane-spanning segment does not cross the membrane.

DISCUSSION

In this study, we report on the membrane topology of the *L. lactis* di- and tripeptide transporter. Since this protein is homologous to a large family of eukaryotic (peptide) transporters, the topology studies have implications for the predicted secondary structure of these proteins as well (see below). To verify the predictions made regarding the locations of the transmembrane segments and their orientation in the membrane, we constructed and analyzed gene fusions of *dtpT* with alkaline phosphatase (*phoA*). The results obtained from several fusions are not in agreement with the predicted secondary structure model of DtpT, in particular regarding the N- and C-terminal TMSs (Figure 1B). For the analysis, we assume that a high PhoA activity corresponds to a periplasmic location and/or a location of the fusion point in the outer leaflet of the membrane. Fusions with intermediate activities are positioned in the middle of the membrane, whereas low PhoA activities are assumed to reflect a fusion point in the cytoplasm or one in the inner leaflet of the membrane. Using these criteria, a residue number of 19 for the TMSs and an overall hydrophobicity of >0.5 [based on the algorithm of Eisenberg et al. (1984)], a new structure model can be constructed that is consistent with the experimental data (Figure 4). The revised secondary structure model shows that the polypeptide crosses the membrane 12 times but that several TMSs are in a different position compared to that in the predicted model (Figure 1B), and that the N and C termini are located intracellularly. In the revised model, all fusions with a high alkaline phosphatase activity (except for Y34) are found in external loops or in the outer halves of putative TMSs.

Fusion proteins G54 and T67 exhibit low alkaline phosphatase activities but are predicted to be in a putative periplasmic loop when the algorithm of Eisenberg and the positive inside rule are used. When the algorithm of Klein et al. (1985) is used, the predictions for the carboxyl-terminal part are the same as those obtained by the Eisenberg method, but the TMSs in the amino-terminal part are arranged differently. The model in Figure 1B shows a long hydrophobic stretch from amino acid residue 52 to 103, whereas the algorithm of Klein et al. (1985) predicts more clearly two putative TMSs for this region. The introduction of an extra TMS in this region results in an intracellular location of the amino terminus and a repositioning of the high activity fusions to the outer half of the cytoplasmic membrane (Figure 4). This modification of the membrane topology is strongly suggested by the fusion proteins L12, T13, G19, L22, A27, I30, A36, L37, S41, G54, and T67.

Fusion D461, which is constructed two residues away from the C terminus, exhibits a low alkaline activity, which suggests that, consistent with the new model (Figure 4), the C terminus is located in the cytoplasm; the original model (Figure 1B) predicts that the C terminus is in the periplasm. Fusion protein E430 exhibits intermediate alkaline phosphatase activity, which may be caused by the loss of several positively charged residues in the C-terminal end. Also in other cases, the absence of carboxyl-terminal sequences has lead to anomalous findings in the membrane topology (Boyd & Beckwith, 1989; Lee & Manoil, 1996). The anomalies can result from the fact that basic amino acid residues found in cytoplasmic loop regions play a prominent role as topological determinants. When PhoA is fused to a residue that precedes basic ones, it is less stably localized in the cytoplasm than if it follows these positively charged residues. The former class of fusions may exhibit higher alkaline phosphatase activities than expected. To obtain further support for the suggestion that the C-terminal end is indeed located in the cytoplasm, we constructed a series of single cysteine mutants and assessed the membrane sideness of these residues by labeling studies with MPB. The results obtained from these studies are in accordance with the hypothesis that the C terminus is located in the cytoplasm. Therefore, we conclude that the last predicted transmembrane segment (residues 433−451) of DtpT is not crossing the membrane, although the hydrophobicity and amphipathy of this region are quite high.

Fusion protein L394 exhibits an intermediate alkaline phosphatase activity, which is 2-fold higher than the activity of E430, but is predicted to be located in a cytoplasmic loop (Figure 1B). Using a sliding window of 19 and the algorithm of Eisenberg et al. (1984), the region from 392 to 410 could form a putative TMS (overall hydrophobicity of 0.41). When this region forms TMS XII, residue L394 can

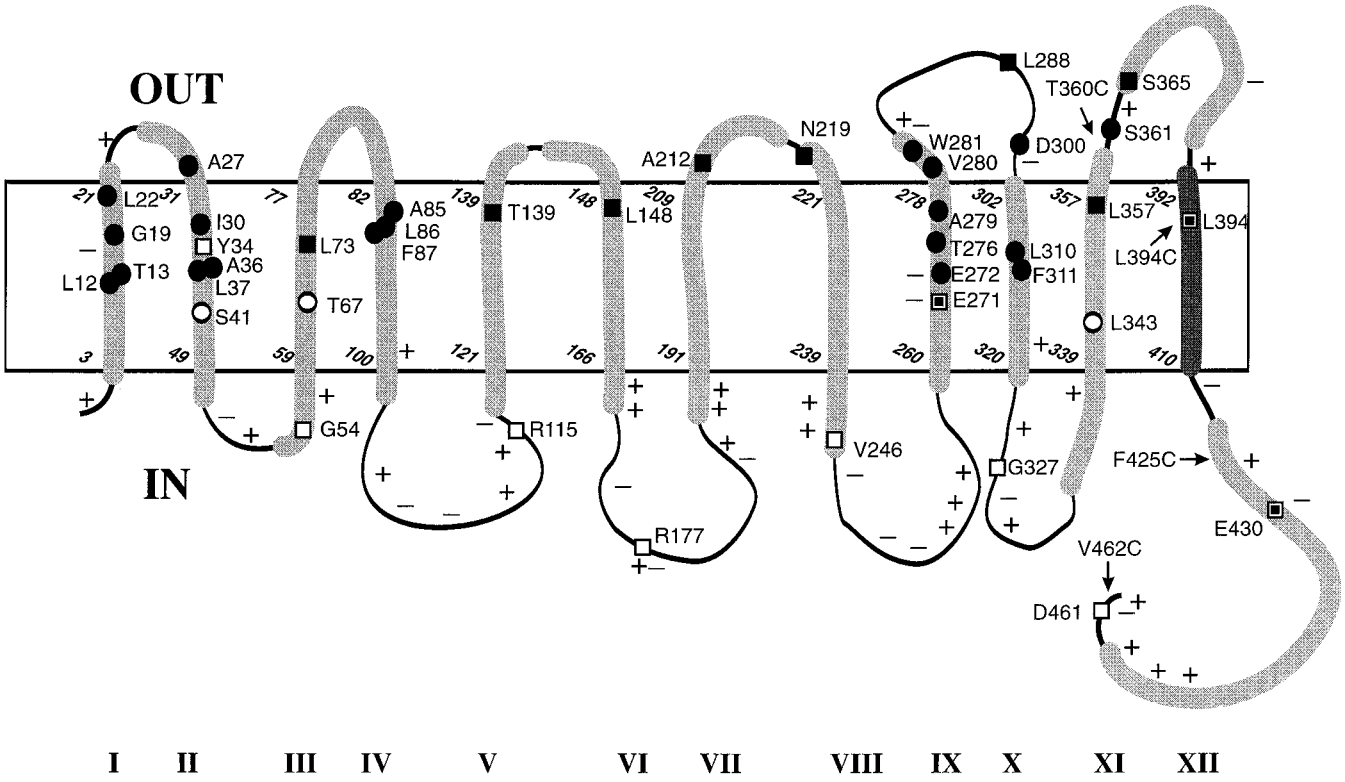

FIGURE 4: Secondary structure model of the di- and tripeptide transport protein DtpT. The model is based on hydropathy profiling, the activity of the DtpT−PhoA fusions, and the labeling pattern of single cysteine mutants. All other symbols are the same as in the legend to Figure 1. The dark shaded stretch indicates a TMS with an overall hydrophobicity of 0.41; the arrows indicate the position at which the single cysteines were engineered.

be accommodated in the periplasmic half of the membrane (Figure 4).

Immunoblot data indicate that the variation in alkaline phosphatase activity of the fusion proteins with their junction points in the periplasmic half of a transmembrane domain or in a periplasmic loop correlates qualitatively with differences in hybrid protein expression. Low-activity fusion proteins are barely or not detected by the Western analysis. Their fusion points are predicted to be in the cytoplasmic half of a TMS or in a cytoplasmic loop These observations are consistent with previous findings (Calamia & Manoil, 1990; Gött & Boos, 1988; Lloyd & Kadner, 1990; Pourcher et al., 1996; Ujwal et al., 1995) and most likely reflect the lack of essential intrachain disulfide bonds, which cannot be formed in the reducing environment of the cytoplasm, thereby making PhoA highly susceptible to proteolytic degradation (Derman & Beckwith, 1991).

In addition to alkaline phosphatase being the positive reporter of a periplasmic location, we have used β-galactosidase as a complementary positive reporter of a cytoplasmic location. The fusion points were identical to those shown in Table 3. Even though the data obtained from the fusions in putative internal loops were entirely consistent with the PhoA data (i.e., high β-galactosidase activities), four DtpT−LacZ fusions, which are most likely in an external loop (L148, N219, L288, and S365), had an unexpected high β-galactosidase activity. In these cases, the liberation of an initially membrane-embedded and enzymatically inactive β-galactosidase portion may have resulted in the formation of active tetramers. In this regard, it is worth noting that these four fusions have a relatively large hydrophilic loop between the last TMS and the LacZ moiety which may have prevented the translocation. Similar anomalies have been observed by others (Chepuri & Gennis, 1990; Eithinger & Friedrich, 1994; Gött and Boos, 1988), which clearly limits the reliability of LacZ as a compartment-specific reporter.

Although sequence comparisons of DtpT and other putative peptide transport proteins have been reported by Steiner et al. (1995), the sequence alignments were not optimized. Moreover, many more homologous proteins have been described in the past years, including three other mammalian peptide transporters (hPepT2 and rbPepT2 from human and rabbit kidney, respectively, and rPepT1 from rat small intestine), two proteins with unknown function from *Caenorhabditis elegans*, a putative nitrate transporter from *Brassica napus* (RCH2), and the products of *yjdL* and *yhiP* in *E. coli*. Recently, we cloned and sequenced the *dtpT* gene of *L. helveticus* (H. Nakajima et al., unpublished results), of which the deduced polypeptide is 34% identical to DtpT of *L. lactis*. Part of the multiple sequence alignment of DtpT and most of its homologues are shown in Figure 5; when sequences are nearly identical, only one of the proteins is shown in the alignment. The alignments were optimized by minimizing the number of gaps. The proposed positions of the TMSs were adjusted in light of the experimental data obtained in this study and predictions made by the algorithm of Eisenberg et al. (1984). The similarity of all members of the PTR family is highest in the N-terminal portion of the proteins, and the membrane topology of DtpT is likely to reflect that of the other proteins as well. There is, however, some ambiguity in assigning the position of TMS I. It is particularly difficult to define TMS I in PTR2, CaPTR2, CePepTa, and AtPTR2B due to the large number of hydrophilic/charged residues throughout the point where

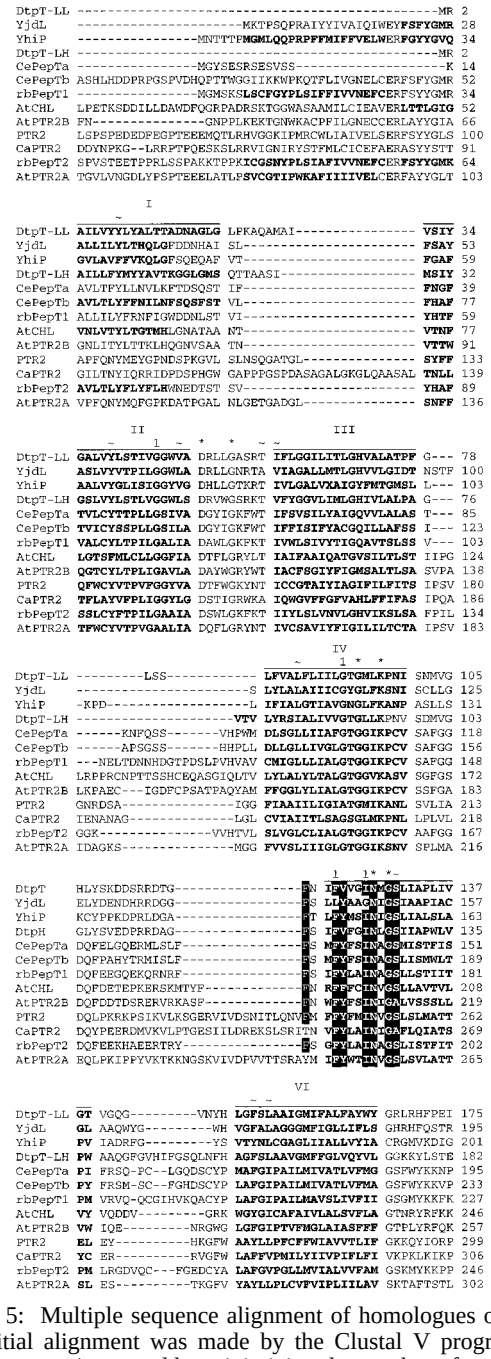

FIGURE 5: Multiple sequence alignment of homologues of DtpT. The initial alignment was made by the Clustal V program; the alignment was improved by minimizing the number of gaps using typical sequence motifs as a guide for the adjustments: *, identical residues; 1, residues conserved in 10 of the 11 protein members; ∼, similar residues; −, gap; horizontal line, position of TMS as inferred from the membrane topology studies (this work); residues in boldface, proposed TMS of members of the PTR family with an overall hydrophobicity of ≥0.43 using a sliding window of 19; residues with a dark background, signature motif of the PTR family. Proteins used are the peptide transporters from *L. lactis* ($DtpT_{LL}$), *L. helveticus* ($DtpT_{LH}$), rabbit small intestine (rbPepT1) and kidney (rbPepT2), *S. cerevisiae* (PTR2), *C. albicans* (CaPTR2), *A. thaliana* (AtPTR2B), a nitrate transporter from *A. thaliana* (AtCHL), and putative proteins from *C. elegans* (CePepT), *E. coli* (YhiP and YjdL). Amino acid sequences from human small intestine (hPepT1) and kidney (hPepT2), from rat (rPepT1), and from *B. napus* (RCH2) were left out of the alignment because these proteins had more than 80% identity with rbPepT1, rbPepT2, rbPepT1, and AtCHL, respectively. The complete sequence alignment is available upon request.

TMS II is indicated (Figure 5). On the basis of the membrane topology of DtpT, we propose that TMS I, as defined in Figure 5, is also present in the eukaryotic members of the PTR family. Although it is energetically unfavorable to have charged residues in the hydrophobic membrane environment, it is possible that these residues in TMS I form ion pairs with residues in other TMSs, thereby stabilizing the overall structure of the protein. Alternatively, these residues may have important catalytic functions, but the poor sequence conservation in this region argues against this possibility.

Hydropathy profiling of the mammalian peptide transporters predicts a large loop of approximately 200 amino acid residues between TMSs IX and X. This loop probably represents the target for N-linked glycosylation and is thus predicted to be extracellular (Fei et al., 1994). This loop region is also present in the *C. elegans* proteins but not in the transporters from yeast (PTR2 and CaPTR2), plant (AtPTR2A, AtPTR2B, and AtCHL), *B. napus* (RCH2), and bacteria. Similarity in sequence and hydropathy is also found in the three C-terminal TMSs of all eukaryotic PTR proteins (not shown), which is suggestive of a similar membrane topology. The prokaryotic proteins, YjdL, YhiP, $DtpT_{LL}$, and $DtpT_{LH}$, are very different from the eukaryotic members of the PTR family in their C-terminal halves. The hydropathy profile of YjdL and YhiP suggests a membrane topology that is very similar to that of DtpT, except that there are additional TMSs predicted in the C-terminal part.

In conclusion, the sequence comparisons suggest that the membrane topology of the members of the PTR family is similar for the N-terminal halves and that the experimental data obtained for DtpT may be used to refine the secondary structure models of the other proteins. The similarity in sequence is highest in the part between TMS II and VI, which also contains the signature motif of the PTR family F-S/T/N/M-X-F-V/Y/F-h-X-I-N-h-G-S/A-h (h indicates a hydrophobic residue). The function of this motif is unknown, but it likely plays an important role in the transport process.

ACKNOWLEDGMENT

The authors thank Hajime Nakajima for making the *L. helveticus* di- and tripeptide transport gene sequence available prior to publication, Dr. Juke S. Lolkema for continuous support, and André Boorsma for assistance in the nucleotide sequencing of the cysteine mutants.

REFERENCES

Basrai, M. A., Lubkowitz, M. A., Perry, J. R., Miller, D., Krainer, E., Naider, F., & Becker, J. M. (1995) *Microbiology 141*, 1147−1156.

Bayer, A. E., Zalis, M. G., & Wilchek, M. (1985) *Anal. Biochem. 149*, 529−536.

Boll, M., Herget, M., Wagener, M., Weber, W. M., Markovich, D., Biber, J., Clauss, W., Murer, H., & Daniel, H. (1996) *Proc. Natl. Acad. Sci. U.S.A. 93*, 284−289.

Boyd, D., & Beckwith, J. (1989) *Proc. Natl. Acad. Sci. U.S.A. 86*, 9446−9450.

Brickman, E., & Beckwith, J. (1975) *J. Mol. Biol. 96*, 307−316.

Calamia, J., & Manoil, C. (1990) *Proc. Natl. Acad. Sci. U. S. A. 87*, 4937−4941.

Chepuri, V., & Gennis, B. (1990) *J. Biol. Chem. 265*, 12978−12986.

Derman, A. I., & Beckwith, J. (1991) *J. Bacteriol. 173*, 7719−7722.

Eisenberg, D., Schwarz, E., Komaromy, M., & Wall, R. (1984) *Annu. Rev. Biochem. 53*, 595−623.

Eithinger, T., & Friedrich, B. (1994) *Mol. Microbiol. 12*, 1025−1032.

Fei, Y.-J., Kanai, Y., Nussberger, S., Ganapathy, V., Leibach, F. H., Romero, M. F., Singh, S. K., Boron, W. F., & Hediger, M. A. (1994) *Nature 368*, 563−566.
Foucaud, C., Kunji, E. R. S., Hagting, A., Richard, J., Desmazeaud, M., & Poolman, B. (1995) *J. Bacteriol. 177*, 4652−4657.
Gött, P., & Boos, W. (1988) *Mol. Microbiol. 2*, 655−663.
Gutierrez, C., & Devedjian, J. C. (1989) *Nucleic Acids Res. 17*, 3999.
Hagting, A., Kunji, E. R. S., Leenhouts, K. J., Poolman, B., & Konings, W. N (1994) *J. Biol. Chem. 269*, 11391−11399.
Higgins, C. F. (1992) *Annu. Rev. Cell Biol. 8*, 67−113.
Klein, P., Kanehisa, M., & DeLisi, C. (1985) *Biochim. Biophys. Acta 815*, 468−476.
Kunji, E. R. S., Hagting, A., De Vries, C. J., Juillard, V., Haandrikman, A. J., Poolman, B., & Konings, W. N. (1995) *J. Biol. Chem. 270*, 1569−1574.
Kyhse-Anderson, J. (1984) *J. Biochem. Biophys. Meth*ods *10*, 203−209.
Lee, M., & Manoil, C. (1996) in *Transport Processes in Eukaryotic and Prokaryotic Organisms* (Konings, W. N., Kaback, H. R., & Lolkema, J. S., Eds.) Vol. 2, pp 189−201, Elsevier Science B. V., Amsterdam.
Liang, R., Fei, Y.-J., Prasad, P. D., Ramamoorthy, S., Han, H., Yang-Feng, T. L., Hediger, M. A., Ganapathy, V., & Leibach, F. H. (1995) *J. Biol. Chem. 270*, 6456−6463.
Liu, W., Liang, R., Ramamoorthy, S., Fei, Y.-J., Ganapathy, M. E., Hediger, M. A., Ganapathy, V., & Leibach, F. H. (1995) *Biochim. Biophys. Acta 1235*, 461−466.
Lloyd, A. D., & Kadner, R. J. (1990) *J. Bacteriol. 172*, 1688−1693.
Loo, T. W., & Clarke, D. M. (1995) *J. Biol. Chem. 270*, 843−848.
Miyamoto, K.-I., Shiraga, T., Morita, K., Yamamoyo, H., Haga, H., Taketani, Y., Tamai, I., Sai, Y., Tsuji, A., & Takeda, E. (1996) *Biochim. Biophys. Acta 1305*, 34−38.
Perry, J. R., Basrai, M. A., Steiner, H.-Y., Naider, F., & Becker, J. M. (1994) *Mol. Cell. Biol. 14*, 104−115.
Poolman, B., & Konings, W. N. (1988) *J. Bacteriol. 170*, 700−707.
Pourcher, T., Bibi, E., Kaback, H. R., & Leblanc, G. (1996) *Biochemistry 35*, 4161−4168.
Sambrook, J., Fritsch, E. F., & Maniatis, T. (1989) *Molecular Cloning: a Laboratory Manual*, 2nd ed., Cold Spring Harbor Laboratory Press, Plainview, NY.
Sanger, F., Nicklen, S., & Coulson, A. R. (1977) *Proc. Natl. Acad. Sci. U.S.A. 74*, 5463−5467.
Song, W., Steiner, H.-Y., Zhang, L., Stacey, G., & Becker, J. M. (1996) *Plant Physiol. 110*, 171−178.
Steiner, H.-Y., Song, W., Zhang, L., Naider, F., Becker, J. M., & Stacey, G. (1994) *Plant Cell 6*, 1289−1299.
Steiner, H.-Y., Naider, F., & Becker, J. M. (1995) *Mol. Microbiol. 16*, 825−834.
Tsay, Y.-F., Schroeder, J. L., Feldmann, K. A., & Crawford, N. M. (1993) *Cell 72*, 705−713.
Ujwal, M. L., Jung, H., Bibi, E., Manoil, C., Altenbach, C., Hubell, W. L., & Kaback, H. R. (1995) *Biochemistry 34*, 14909−14917.
van Geest, M., & Lolkema, J. S. (1996) *J. Biol. Chem. 271*, 25582−25589.
von Heijne, G., & Gavel, Y. (1988) *Eur. J. Biochem. 174*, 671−678.

BI963068T